Available online at www.sciencedirect.com

ScienceDirect

Procedia Computer Science 76 (2015) 95 – 100

Procedia Computer Science

2015 IEEE International Symposium on Robotics and Intelligent Sensors (IRIS 2015)

Sensitivity-Enhancing All-in-type Optical Three-axis Tactile Sensor Mounted on Articulated Robotic Fingers

A. Takagi*[a], Y. Yamamoto[a], M. Ohka[a], H. Yussof[b], S. C. Abdullah[b]

[a]*Graduate School of Engineering, Nagoya University, Furo-cho, Chikusa-ku, Nagoya 464-8603, Japan*
[b]*Center for Humanoid Robots and Bio-Sensing (HuRoBs), Faculty of Mechanical Engineering, Universiti Teknologi MARA, Malaysia*

Abstract

In a previous study, we developed an all-in-type optical three-axis tactile sensor to address two issues: the first is to be able to use external devices such as a CCD camera and light source; the other is the insensible zone. We miniaturized its whole structure through adoption of a CMOS board camera equipped with LEDs. Since a USB is installed in the CMOS camera as an interface, an additional image processing board is not required. Furthermore, it is equipped with a rubber dome including a sensing element array to remove the insensible zone because rubber is filled in between the sensing elements. However, even if it accepted under around 1-N force, no output of brightness appeared. In this paper, we enhance the characteristic in the low level applied force through improvement of image processing. Furthermore, the present sensor showed higher output level of normal and tangential forces through a series of experiments comparing the present and ordinal three-axis tactile sensors.

Peer-review under responsibility of organizing committee of the 2015 IEEE International Symposium on Robotics and Intelligent Sensors (IRIS 2015)

Keywords: Robotic tactile sensor; All-in-type; Sensitivity enhancement; Rubber dome structure; Robotic finger

1. Introduction

For intelligent robots, tactile information is very important for handling an unknown object because they need several kinds of mechanical information such as hardness, roughness and shape of the object.[1] Since three-axis

* Corresponding author. Tel.: +81-52-789-4861; fax:+81-52-789-4800.
*E-mail address:*ohka@is.nagoya-u.ac.jp

Peer-review under responsibility of organizing committee of the 2015 IEEE International Symposium on Robotics and Intelligent Sensors (IRIS 2015)
doi:10.1016/j.procs.2015.12.286

tactile sensors capable of sensing not only normal force but also tangential force distributions are effective for evaluating mechanical properties of an object, several kinds of three-axis tactile sensors have been developed.[2-5] In particular, three-axis tactile sensors based on image data processing are excellent candidates for achieving robotic tasks intelligently and stably because they have robust characteristics such as resistance to external noise and durability against impact force, which cause fatal damage in performing tasks. Thus far, our tactile sensors have been applied to a dual arm robot to prove the effectiveness of this sensor in advanced robotics.[6-8]

However, our tactile sensor has two problems related to compactness and sparse-element-configuration; the former is caused by wiring to several external devices such as a camera, a fiber scope, a lens system, an image board and a light source; the latter results from its sensing elements being sparsely distributed on the sensor surface. In particular, the problems related to the former become more serious because electric and optical cables connecting the external devices prevent the robot from being manipulated freely. The latter problem was already solved through a new design of a rubber dome including sensing elements.[9] Furthermore, in our previous work,[10] we produced a new all-in-type tactile sensor, which included a camera board, LED light source and USB interface in its casing for solving the former problem. Although our sensor was able to solve the above problems, it still had a problem in that it could not measure below around 1-N force.

In this paper, we enhance the characteristic in the low level applied force through improvement of image processing. Furthermore, the present tactile sensor shows higher outputs for normal and tangential forces through a series of experiments comparing the present tactile sensor and ordinal three-axis tactile sensor.

2. Sensor Designs

2.1. Basic Sensing Principle of Image-Based Tactile Sensor

The basic structure of the image-based tactile sensor is comprised of a rubber sheet and a transparent acrylic plate illuminated along its edge by a light source. The light, which is directed into the plate, remains within it due to the total internal reflection that is generated. A rubber sheet featuring an array of conical feelers is placed on the plate to maintain array surface contact with the plate. If an object contacts the back of the rubber sheet, resulting in contact pressure, the feelers collapse and, at the points where they collapse, light is diffusely reflected out of the plate's reverse surface. The distribution of the contact pressure is calculated from the bright areas viewed from the reverse surface of the plate. Next, we introduce two tactile sensors: the all-in-type three-axis tactile sensor and the ordinal optical three-axis tactile sensor. Both are designed based on the above image-based tactile sensor.

2.2. All-in-type Three-axis Tactile Sensor

The ordinal three-axis tactile sensor explained in the last section proved effective at allowing an advanced robot to perform certain tasks intelligently and stably, including cap-twisting, object-passing and object-assembling.[6-8] However, the ordinal tactile sensor has several problems related to compactness and sparse-element-configuration. The former is caused by wiring to several external devices such as a camera, a fiber scope, a lens system, an image board and a light source. The latter is caused by its sensing elements being sparsely distributed on the sensor surface. In particular, the problems related to the former become more serious because electric and optical cables connecting the external devices prevent the robot from being manipulated freely. In this paper, we intend to solve the former problem because we will apply the robot equipped with the three-axis tactile sensors to a wider field in terms of optical-cableless structure.

Figure 1 shows the design of a new three-axis tactile sensor to solve the former problem. While in the ordinal sensor image data are retrieved via the fiberscope and sent to an external image board installed in a computer, in the new tactile sensor the image data are retrieved by an on-board camera. Since the on-board camera has LEDs on the board (Fig. 2), an external light source is not required.

In the new tactile sensor, a rubber dome is used as shown in Fig. 3. In the rubber dome, two kinds of rubber are used: one of them is hard rubber for the sensing element; the other is soft rubber for skin. Since the skin is softer than the sensing element, not only is the sensing element pushed according to the normal component of force, but the sensing element's attitude can also be changed according to the tangential component of force as shown in Fig. 3.

Normal and tangential force components are measured by brightness of contact area and movement of contact area. Thus, normal and tangential forces are measured from an integrated brightness of the image data G and the centroid movement of the bright area, which is expressed by u_x and u_y in local coordinates. We assume that three components of applied force, F_x, F_y, and F_z, are proportional to u_x, u_y, and G.

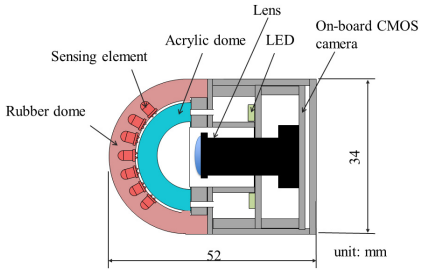

Fig. 1. All-in-type three-axis tactile sensor (Sensor A)

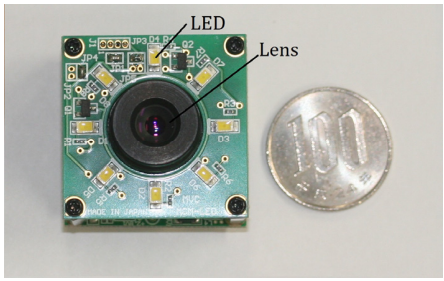

Fig. 2 LED configuration of on-board CMOS camera

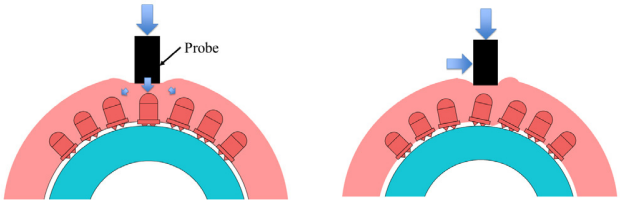

Fig. 3. Sensing mechanism: (a) normal force, (b) tangential force

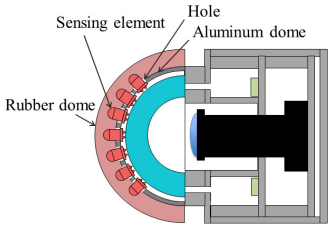

Fig. 4 Covered ordinal optical three-axis tactile sensor (Sensor B)

2.3. Covered Ordinal Optical Three-axis Tactile Sensor

Since the original optical three-axis tactile sensor did not have a rubber dome, sensing elements are supported by an aluminum dome. In the sensor, sensing elements are inserted into holes on the aluminum dome. If a rubber skin is attached to the ordinal optical three-axis tactile sensor, it becomes the covered ordinal optical three-axis tactile sensor (Sensor B)[9] shown in Fig. 4. Although the difference between Sensors A and B is only possessing an aluminum dome or not, it is not elucidated how the difference affects sensing characteristics caused by it.

3. Image Processing to Obtain Tactile Data

In this sensor, we obtain brightness and centroid occurring in each sensing element from image data. For image data processing, we used Microsoft Visual Studio 2012 and the library of OpenCV 2.4.9. After image data (640×480 pixels) are captured by the on-board CMOS camera, normal and tangential forces are calculated from brightness summation and centroid movement, respectively. The calculation flow is shown in Fig. 5.

Since this tactile sensor has 41 elements, the flow should be performed for each region of elements. To perform this, we use a Region Of Interest (ROI) process incorporated in the library because data of a specific area are used in this sensor. Figure 6 shows regions processed for ROI (50×50 pixels) in which the top left corner is designated as the origin; x- and y-axes are right and down directions. Brightness summation and centroid movement of each ROI are calculated. To obtain the brightness and centroid in the specific ROI, we used cvSum and cvGetSpatialMoment of functions included in OpenCV, respectively.

In the preceding paper[10], since image data captured by the CMOS camera included noise, we assumed a threshold for image data, and the pixels of image data were quantized as 0 or 1 to avoid the noise. Although this procedure made the image data clear, it abandoned small brightness under the threshold. Therefore, the quantization process is excluded in this paper.

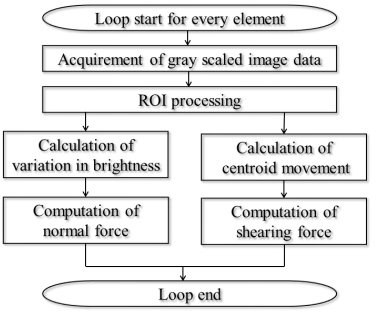

Fig. 5. Flowchart of tactile data calculation

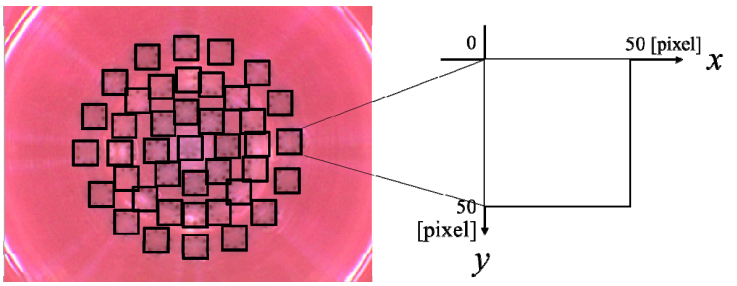

Fig. 6 ROI of tactile sensing elements

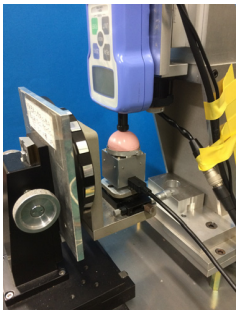

Fig. 7. Normal force test

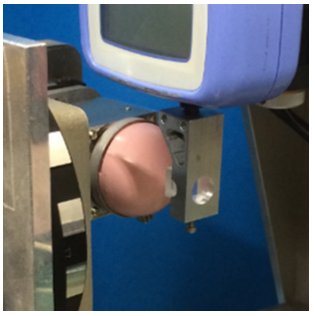

Fig. 8 Tangential force sensing

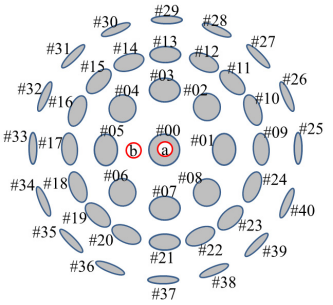

Fig. 9 Loading points of normal force procedure

4. Experimental Results and Discussion

4.1. Experimental Setup and Procedure

To evaluate the present tactile sensor, we used an apparatus machine capable of applying a combined load of normal and tangential forces. The apparatus is composed of a digital force gauge (FGP-1, NIDEC-Simpo Co.), a motorized *z*-table (VSQ-601X, Chuo Precision Industrial Co.; this table is vertically used as a *z*-table), rotary tables (RS-112, Chuo Precision Industrial Co.) and an *x*-*y* table (LS-21-C1, Chuo Precision Industrial Co.) as shown in Fig. 7. In this apparatus, using rotary tables and the *x*-*y* table, any combination of normal and tangential forces can be applied to any position of the sensing surface within the ranges of the rotary table and the *x*-*y* table. Since the digital force gauge can measure net force of 10 N with resolution of 0.01 N, the apparatus can measure sensing characteristics of the present tactile sensor under 0 – 10 N. Configurations for normal and tangential force tests are shown in Figs. 7 and 8, respectively.

For the normal force test, normal force is applied through the probe of the force gauge as shown in Fig. 7. Since both Sensors A and B can measure a force applied between sensing elements, the force is applied to not only Point “a” but also Point “b” shown in Fig. 9. For tangential force sensing, after the sensor axis is rotated within 90°, normal force is applied to the parietal portion through the *x*-*y* stage. At that time, the value of applied normal force is measured by output of the tactile sensor. Maintaining the normal force constant, tangential force is applied to the parietal of the tactile sensor using the motorized *z*-table. The applied tangential force is measured by the force gauge.

4.2. Normal Force Sensing

To evaluate the present tactile sensor (Sensor A), we examine the results of the normal force test to compare the result for Sensor A with that of Sensor B. Figure 10 shows experimental results of the normal force test when force

is applied to Point a, which is the parietal portion of the sensor. First, if the result of Fig. 10(a) is examined, we notice that the output of Sensor A arises after 0 N. This result is completely different from the preceding results, which showed around 1-N insensible force region. Improved data processing described in Chapter 3 successfully accomplishes the diminution of the insensible force region. However, the nonlinear variation in brightness such as the "S" shape is more salient than that of Sensor B shown in Fig. 10 (b). Although the output of brightness between 1 N to 4 N of Sensor A is greater than that of Sensor B, the output of element #0 interfered with surrounding elements #1 to #8. This interference is more salient than that of Sensor B.

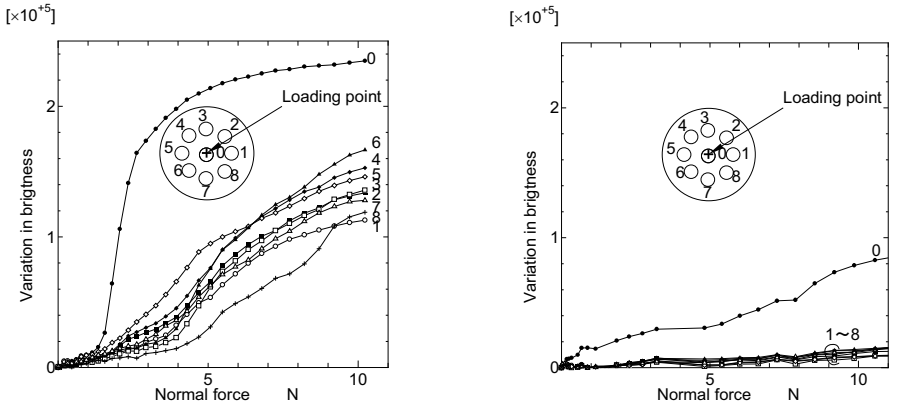

Fig. 10. Experimental results of normal force test when force is applied to Point a: (a) Sensor A, (b) Sensor B

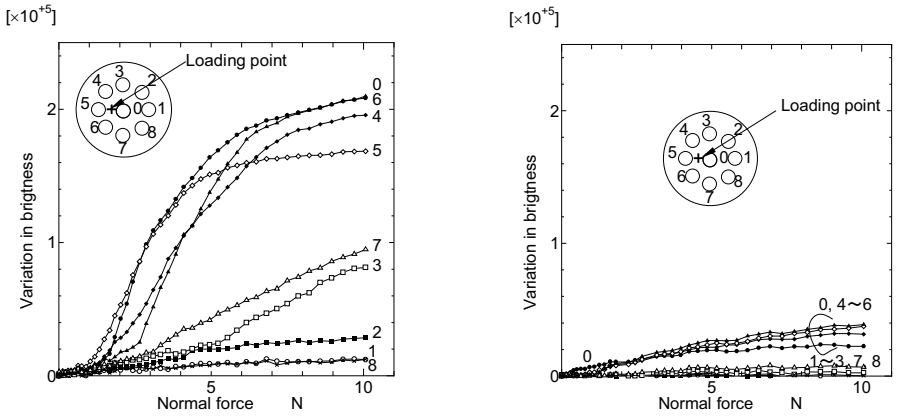

Fig. 11. Experimental results of normal force test when force is applied to Point b: (a) Sensor A, (b) Sensor B

Next, since both Sensors A and B can measure the force applied between elements, we examine this in Fig. 11. Since outputs of elements #0, #4 – #6 surrounding Point b increase in both (a) and (b), from the viewpoint of the sensible zone, Sensors A and B have similar characteristics.

4.3. Tangential Force Sensing

Figure 12 shows the relationship under three kinds of normal force (1, 2 and 3 N). In Fig. 12(a), centroid movement is proportional to shearing force. Compared to behavior of brightness having undulating variation with normal force change, we notice that centroid movements of 1 – 3 N almost linearly vary, and inclination of the 3-N case is slightly different from the 1- and 2-N cases. Furthermore, variation in brightness keeps almost constant for

1–3 N shown in 12 (b). Therefore, although Sensor A has a problem related to precision, it can separately accept normal and shearing force.

On the other hand, we could not observe any centroid movement of Sensor B. If we consider that even the sensor structure of Sensor B obtained a fine result in the previous study,[9] the structure of Sensor B is not suitable for the present CMOS camera, which does not have the same sensitivity as the CCD camera used in the previous study. Since reflective ability of the rubber dome is stronger than the sensing element, and the rubber dome backside maintains contact with the acrylic dome under compressive force, Sensor A shows enough shearing force sensitivity but Sensor B does not.

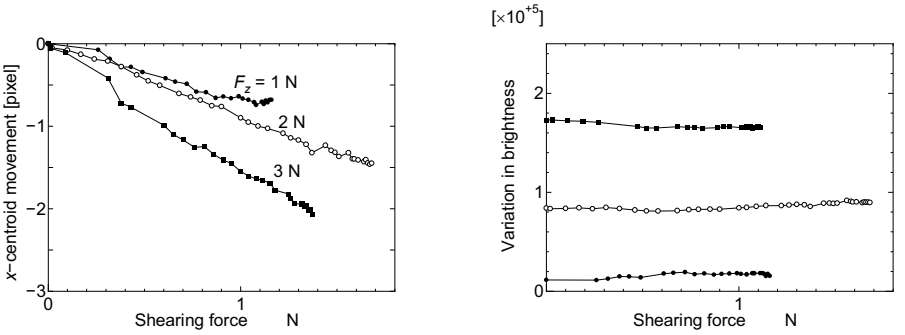

Fig. 12. Experimental results of shearing force test when force is applied to Point a: (a) centroid movement, (b) brightness

5. Conclusion

To advance the all-in-type tactile sensor, we improved the software for tactile data processing and obtained its sensing characteristics. The improved software reduced the insensible force region under 1 N. Furthermore, a comparative experiment between the new design of the rubber dome and the ordinal design of aluminum and rubber domes showed that the former design caused larger output than the latter. Although the new design of the rubber dome provided larger output of brightness than the ordinal design, it provided considerably large nonlinearity and larger interference between sensing elements. However, it has an advantage in that it does not require optical fibers for image data and light source. Since this advantage is essential for active behavior of robots, we will improve the all-in-type tactile sensor to include it in future work.

References

1. M. Ohka, Robotic Tactile Sensors, *Wiley Encyclopedia of Computer Science and Engineering*（Editor: B. W, Wah); 2009, **4**, pp. 2454-2461.
2. Y. Yamada and M. R. Cutkosky, Tactile Sensor with 3-axis Force and Vibration Sensing Function and Its Application to Detect Rotational Slip, *1994 IEEE International Conference on Robotics and Automation*; 1994, pp. 3550-3557.
3. K. Kamiyama, K. Vlack, T. Mizota, H. Kajimoto, N. Kawakami, S. Tachi, Vision-Based Sensor for Real-Time Measuring of Surface Traction Fields, *IEEE Computer Graphics and Applications*; 2005, pp. 68-75.
4. Y. Tanaka, A. Nakai, E. Iwase, T. Goto, K. Matsumoto, and I. Shimoyama, Triaxial Tactile Sensor Chips with Piezoresistive Cantilevers Mountable on Curved Surface. *Proceedings of the 4th Asia Pacific Conference on Transducers and Micro/Nano Technologies*; 2008, 1B1-1.
5. M. Hamidullah, M. Cheng, L. S. Lim, C. He, H. Feng, and W. Park, MEMS Tri-axial Tactile Sensor Packaging Using Polymer Flexible Cable for Sensorised Guide Wire Application, *2011 IEEE 13th Electronics Packaging Technology Conference (EPTC)*; 2011, pp. 207-210.
6. M. Ohka, J. Takata, H. Kobayashi, H. Suzuki, N. Morisawa, and H. Yussof, Object Exploration and Manipulation Using a Robotic Finger Equipped with an Optical Three-axis Tactile Sensor, *Robotica*; 2009, **27-5**, pp. 763-770.
7. M. Ohka, S. C. Abdullah, J. Wada and H. B. Yussof, Two-hand-arm Manipulation Based on Tri-axial Tactile Data, *International Journal of Social Robotics*; 2012, **4-1**, pp. 97-105.
8. M. Ohka, H. Kobayashi, J. Takata, and Y. Mitsuya, An Experimental Optical Three-axis Tactile Sensor Featured with Hemispherical Surface, *Journal of Advanced Mechanical Design, Systems, and Manufacturing*; 2008, **2(5)**, pp. 860-873.
9. M. Ohka, A. Tsunogai, T. Kayaba, S. C. Abdullah and H. Yussof, Advanced Design of Columnar-conical Feeler-type Optical Three-axis Tactile Sensor, *Procedia Computer Science*; 2014, **42**, pp. 17-24.
10. M. Ohka, Y. Yamamoto, H. Yussof and S. C. Abdullah, All-in-type Optical Three-axis Tactile Sensor, *2014 IEEE International Symposium on Robotics and Manufacturing Automation*; 2014, pp. 79-84.